International Journal of Energy
ISSN: 2957-9473 | Vol. 9, No. 1, 2026

Study of Expansion Force Distribution during Lithium-ion Battery Operation and Ageing

Jinrong Xu *, Yang Yang, Mingzhi Ye

Hefei Gotion High-tech Power Energy Co., Ltd., Hefei, Anhui, China

* **Corresponding author**: Jinrong Xu (Email: m13127820212@163.com)

Abstract: In the process of battery charge-discharge and long-term aging, a novel customized thin-film pressure sensor system was used to directly measure the swelling force of prismatic cells, providing insights into the electrode swelling mechanism inside lithium-ion batteries. Battery electrical performance data were obtained from cycle charge-discharge tests and capacity calibration tests conducted at every 50 aging cycles interval, while battery state of health data were collected over a total of 1000 cycles. Using a prismatic cell equipped with thin-film pressure sensors, key characterization parameters such as battery current, battery voltage, calibrated capacity discharged at 1C current, and the regional distribution of expansion force during charge-discharge in cycling aging were recorded. These data provide an understanding of the internal electrode swelling in prismatic cells and reveal the inherent coupling relationship among the state of charge, state of health, and the variation and distribution of expansion force. The published dataset offers a valuable resource for enhancing battery diagnostics and developing data-driven models to estimate state of charge (SOC) and state of health (SOH), which can be used for advanced battery safety monitoring and the construction of multi-feature fusion diagnostic models for battery failure. The provided data deepen the fundamental understanding of the variation mechanism of internal electrode expansion force in prismatic cells during operation and aging. Since data on electrode expansion force for the prismatic cell have not been publicly available, the provided dataset fills a gap in existing open data collections.

Keywords: Expansion Force; In-situ Monitoring; Ageing; Advanced Characterization; SOH; Thin-film Pressure Sensor.

1. Introduction

This experiment aims to deepen the understanding of electrode swelling behavior during the operation of lithium-ion batteries by investigating the influence of battery SOC and SOH on the distribution and variation of battery expansion force. In recent years, with the increasingly widespread application of lithium batteries, there is a growing demand for higher safety performance and cycling performance. At the same time, the risks and pollution caused by lithium battery thermal runaway have raised concerns [2]. During the charge-discharge process, lithium batteries exhibit swelling behavior, which not only poses serious safety hazards but also reduces their cycle life.

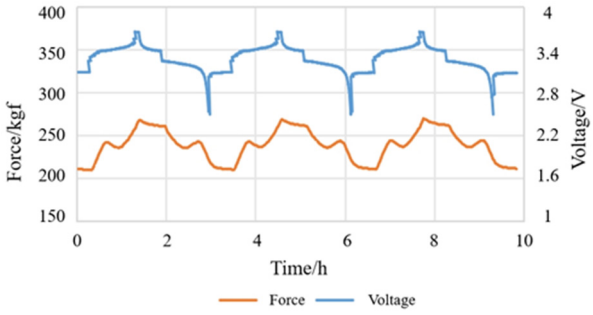

Figure 1. The expansion force during charging and discharging

How to quickly and accurately measure the expansion force of battery cells has attracted increasing attention in the industry [3]. During battery charge-discharge cycles, active lithium forms an SEI layer at the graphite anode interface, and the resulting by-products accumulate at the interface, leading to an overall increase in battery thickness [4]. Taking the three-cycle charge-discharge process of a battery cell as an example, the variation in expansion force and its corresponding voltage changes are illustrated in Figure 1.

This expansion force dataset can be used to monitor and provide early warnings of abnormal swelling during battery charge and discharge processes, thereby avoiding performance degradation or even thermal runaway risks caused by the accumulation of mechanical stress due to volume changes [5]. By analyzing the distribution of force or thickness changes on the tested surface of the battery during the testing process, it enables accurate identification and detection of expansion force variations in key areas. This provides technical references for setting the venting pressure of burst disks and designing the safety structure of battery modules [6].

2. Experimental Design and Methods

Table 1. Technical specification for battery

Item	Specification	Unit
Format	40*148*88	mm
Rated capacity	53	Ah
Mass	3.15	V
Nominal voltage	3.65	V
Charge cut-off voltage	2.5	V
Discharge cut-off voltage	-20~55	℃
Operating temperature	-35~60	℃
Cathode	LiFePO4	-
Anode	LiC6	-
Separator	Ceramic-coated	-

The experimental dataset includes one prismatic cell (Gotion-IFP4014888-53Ah) and one 1P10S module composed of 10 such prismatic cells connected in series. Both underwent 1000 cycles of aging, with capacity calibration performed once every 50 cycles. The cell technical

parameters are listed in Table 1.

Place the battery or module to be tested into the test fixture, which includes a combined clamping and pressurizing tooling as well as a detection device. Measure the expansion force or displacement variation during battery testing through constant-gap expansion force testing. Position the expansion force fixture inside an environmental chamber set to the target temperature, connect the pressure sensor to the data acquisition unit and monitoring system, and then adjust the preload force to the target value based on the monitoring system. The experimental setup is shown in Figure 2.

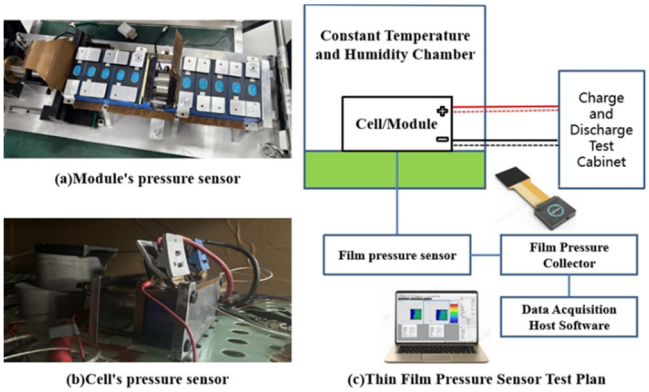

Figure 2. The Test Equipment Connection Diagram

The initial force on the test sample before adjustment is zero. Adjust the preload force to the target set value of 200 kgf. To avoid damaging the sample due to sudden excessive pressure, each adjustment during the application of force should not exceed an increase of 50 kgf.

The battery underwent room-temperature cycling tests and capacity calibration tests, during which the distribution and variation of expansion force were monitored. All cycling and characterization experiments were conducted inside a Constant Temperature and Humidity Chamber (model ECT-960DU-45-TP-AR). The test procedures were programmed using Scienlab software, and the charge-discharge processes for both the cell and module were performed by a charge-discharge test cabinet (model PSC60-600), which also collected and recorded parameters such as voltage, current, capacity, and energy. The surface temperature of the cell was measured by a K-type thermocouple (model HEL014239) attached to its center, with data recorded by a CPR-ST03D data logger. The expansion force was captured using a Tisun thin-film pressure sensor (model SA6464-22A-HP) along with its dedicated pressure acquisition unit (model DH1-A10), and logged via supporting software.

The cycling procedure is detailed in Table 2, and the capacity calibration procedure is outlined in Table 3. Both the cell and the module (with adjusted charge-discharge current and voltage parameters based on its configuration) followed the procedures specified in Table 2 and Table 3 for cycle aging and capacity calibration.

Table 2. Ageing protocol

Step	Mode	Action	Limits	Description
1	Capacity Calibration	(See Table 3)		
2	Rest		23°C≤T≤27°C	Temperature control
3	1C Discharge	CC 1C = 53A	V ≤ 2.5 V	1C Discharge to 0 % SOC
4	Rest		23°C≤T≤27°C	Temperature control
5	2C Charge	CC 2C = 106A	C≥20%C0/V ≥ 3.65 V	2C Charge to 20% SOC
6	1.8C Charge	CC 1.8C = 95.4A	C≥40%C0/V ≥ 3.65 V	1.8C Charge to 40% SOC
7	1.6C Charge	CC 1.6C = 84.8A	C≥60%C0/V ≥ 3.65 V	1.6C Charge to 60% SOC
8	1.4C Charge	CC 1.4C = 74.2A	C≥70%C0/V ≥ 3.65 V	1.4C Charge to 70% SOC
9	1.2C Charge	CC 1.2C = 63.6A	C≥80%C0/V ≥ 3.65 V	1.2C Charge to 80% SOC
10	0.8C Charge	CC 0.8C = 42.4A	C≥90%C0/V ≥ 3.65 V	0.8C Charge to 90% SOC
11	0.5C Charge	CC 0.5C = 26.5A	C≥95%C0/V ≥ 3.65 V	0.5C Charge to 95% SOC
12	0.25C Charge	CC 0.25C = 13.25A	C≥99%C0/V ≥ 3.65 V	0.25 Charge to 99% SOC
13	0.1C Charge	CC 0.1C = 5.3A	C≥100%C0/V ≥ 3.65 V	0.1C Charge to 100% SOC
14	Rest		23°C≤T≤27°C	Temperature control
15	1C Discharge	CC 1C = 53A	V < 2.5 V	1C Discharge to 0% SOC
16	Loop	Go to Step 4	50 times	Repeat cycle
17	Capacity Calibration	(See Table 3)		

Table 3. Capacity calibration protocol

Step	Mode	Action	Limits	Description
1	Rest		23°C≤T≤27°C	Temperature control
2	1C Discharge	CC 1C = 53A	V ≤ 2.5 V	1C Discharge to 0 % SOC
3	Rest		Time: 0.5 h	
4	Rest		23°C≤T≤27°C	Temperature control
4	Charge	CC 1C = 53A CV 3.65V	V≥3.65V I≤2.65A	CC-CV Charge to 100 % SOC
5	Rest		Time: 0.5 h	
6	Rest		23°C≤T≤27°C	Temperature control
7	1C Discharge	CC 1C = 53A	V ≤ 2.5 V	1C Discharge to 0 % SOC
8	Loop	Go to Step 3	3 times	Repeat cycle, the average value of the three discharge capacities is C0

3. Conclusion

By visualizing the numerical matrix of the expansion force distribution on the main surface of the battery, the magnitude distribution of the expansion force at key SOC points during the charge and discharge phases can be directly observed, as shown in Figure 3.

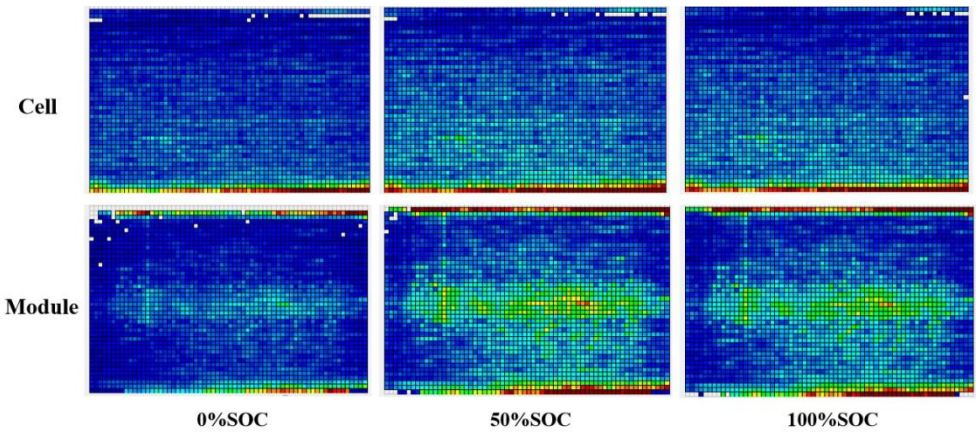

Figure 3. Expansion force distribution during the 400th cycle charging process for both the cell and the module

The expansion force visualizations in the figures are taken from the expansion force distribution at 0% SOC, 50% SOC, and 100% SOC points during the charging process of the 400th cycle aging for both the cell and the module. The figures reveal that due to surface unevenness, the pressure is higher at the top and bottom of the cell and module. As cycling progresses, the middle of the cell begins to swell, partially offsetting the pressure in the top and bottom regions. These observations provide more detailed and specific analytical features for the coupled analysis of SOC and expansion force distribution, thereby enhancing the potential for improved prediction accuracy.

The data enhances the understanding of expansion force variations during charge-discharge and cycling processes in prismatic cells. Currently, there is no publicly available data on the distribution and changes of expansion force for Gotion-IFP4014888-53Ah, and this dataset fills that gap.

The data reveals the influence of battery SOH on the distribution and variation of expansion force, which can be used to further study the patterns of expansion force changes with battery SOH, optimize SOH estimation algorithms [1], and help elucidate the swelling mechanism of electrodes during cycling. This data supports innovation in battery diagnostics and provides robust data support for failure analysis, structural optimization, and safety evaluation of batteries through distributed multidimensional force monitoring.

By incorporating expansion force characteristics, the data integrates multi-feature data fusion algorithms to improve the accuracy of SOC estimation. This work provides a novel, practical, and accurate dataset of features for SOC estimation algorithms in batteries for electric vehicles and energy storage systems

References

[1] Chen G ,Zhou H ,Yang J , et al.Optimization of open-circuit voltage curve acquisition and state estimation for aging lithium-ion batteries[J].Energy,2026,342139606-139606, doi: 10. 1016/J.ENERGY.2025.139606.

[2] Ivano W.Aiello, Charlie Endris, Steven Cunningham, Monique Fountain, Maxime M.Grand, et al.Coastal wetland deposition of cathode metals from the world's largest lithium-ion battery fire[J].Scientific Reports,2025,15(1):42113-42113, doi:10. 1038/ S41598-025-25972-8.

[3] Wang L ,Li Y ,Tian Y , et al.Early-Stage Fault Diagnosis for Batteries Based on Expansion Force Prediction [J]. Energies, 2025, 18(24):6619-6619, doi:10.3390/EN18246619.

[4] Lou H L ,Liang T X ,Jiang J , et al.A fused electrical-mechanical model with extended Kalman filter and adaptive weighting for state-of-charge estimation of lithium iron-phosphate batteries[J].eTransportation,2026,27100522-100 522, doi: 10. 1016/J.ETRAN.2025.100522.

[5] Senrong Wei, Jianhua Du, Haobin Liang, Canxiong Wang, et al.Study on Thermal Runaway Behavior and Early Warning Algorithm of Ternary Lithium Battery Pack Under Preload Force[J].Energy Technology,2024,12(12):2401238-2401238, doi:10.1002/ENTE.202401238.

[6] Zhou G ,Zhao J ,Zhang S , et al.Stage-specific gas generation dynamics and laminar flame characteristics of mixed gases during full-cycle thermal runaway in 104 Ah prismatic LiFePO4 batteries[J].Fuel,2026,411137978-137978, doi:10. 1016/ J.FUEL.2025.137978.